Nonmethane hydrocarbons in the transported and local air masses at a clean remote site on Hainan Island, south China

Jian-Hui Tang,[1] Lo-Yin Chan,[1] Chuen-Yu Chan,[1] Yok-Sheung Li,[1] Chih-Chung Chang,[2] Shaw-Chen Liu,[2] and Yi-De Li[3]

Received 17 July 2006; revised 30 October 2006; accepted 3 April 2007; published 31 July 2007.

[1] Nonmethane hydrocarbons (NMHCs) were investigated in a clean remote tropical rain forest site of Jianfengling Natural Reserve in Hainan Island in spring, autumn and early winter of 2004. The aim was to characterize air pollution transported from east Asia and SE Asian subcontinent on this relatively undeveloped region of south China. Ethane, ethyne, isoprene and ethene are the most abundant hydrocarbons. The relative contributions of pollution transport from urban and industrial zones of east Asia and agricultural zones of SE Asia are discussed with the help of backward air trajectories. The air masses from the SE Asian biomass burning region contained higher concentrations of ethane and ethyne while air masses traveling through coastal east China contained higher concentrations of ethene and toluene in addition to ethane and ethyne. It was found that anthropogenic emissions transported from the SE and south China developed and developing regions in autumn had a higher input than biomass burning emission from SE Asia in spring. Local biogenic emission was deduced to be the major source of isoprene. Hydrocarbon concentration ratios were found to be good indicators for identification of inflow air masses from different source regions.

Citation: Tang, J.-H., L.-Y. Chan, C.-Y. Chan, Y.-S. Li, C.-C. Chang, S.-C. Liu, and Y.-D. Li (2007), Nonmethane hydrocarbons in the transported and local air masses at a clean remote site on Hainan Island, south China, *J. Geophys. Res.*, *112*, D14316, doi:10.1029/2006JD007796.

1. Introduction

[2] Nonmethane hydrocarbons (NMHCs) play critical roles in atmospheric chemistry. They are important ozone precursors. Their reactions with the hydroxyl radical (OH) produce many oxygenic compounds, and result in the formation of ozone in the atmosphere. It was estimated that NMHCs contributed about 40% of the total global net photochemical ozone production [*Houweling et al.*, 1998]. The oxidation of NMHCs significantly influences the tropospheric concentrations and budgets of O_3, OH, CO and NOx [*Poisson et al.*, 2000]. The reactions of NMHCs with OH affect the global distribution of OH and subsequently the lifetime of other trace species in the atmosphere [*Poisson et al.*, 2000].

[3] Eastern China is an important source region of anthropogenic pollutants, whereas Southeast Asia is an important source region of biomass burning emission [*de Gouw et al.*, 2004]. Export of pollution from these regions arouses increasing scientific interest in recent years. With the rapid agricultural development, urban expansion and industrialization in China, tremendous amount of anthropogenic air pollutants are emitted into the atmosphere, resulting in rapid deterioration of the air quality of the region and its neighboring western Pacific region [*Chan et al.*, 2000, 2003; *Wang et al.*, 2003]. Biomass burning is an important source of global trace gases and aerosols. It had been estimated that biomass burning emitted about 38.0 Tg NMHCs in 2000 [*Ito and Penner*, 2004]. Southeast Asia is a major biomass burning region associated with active natural and human activated fires during the spring time (February–April) [*Duncan et al.*, 2003; *Heald et al.*, 2003; *Streets et al.*, 2003a, 2003b]. The trace gases and aerosols emitted from the biomass burning activities in SE Asia could be lifted up to the free troposphere and transported through the western Pacific and eventually crossed the Pacific Ocean to North America [*Chan et al.*, 2000; *Jacob et al.*, 2003; *de Gouw et al.*, 2004]. Extensive measurements of NMHCs in the east Asia–western Pacific region had been carried out by aircraft during several large-scale field campaigns, such as the Pacific Exploratory Mission–West expedition phase A and phase B (PEM-West A and PEM-West B) and the Transport and Chemical Evolution Over the Pacific (TRACE-P) [*Blake et al.*, 1996, 1997, 2003]. Several ground level measurements had also been conducted in rural and remote sites of Japan [*Sharma et al.*, 2000; *Kato et al.*, 2001] and rural sites of Hong Kong [*Wang et al.*, 2003, 2005]. However, there were little NMHCs data reported for remote regions of mainland China. This paper

[1]Department of Civil and Structural Engineering, Hong Kong Polytechnic University, Hung Hom, Kowloon, Hong Kong.
[2]Research Center for Environmental Changes, Academia Sinica, Taipei, Taiwan.
[3]Research Institute of Tropical Forestry, Chinese Academy of Forestry, Guangzhou, China.

0148-0227/07/2006JD007796

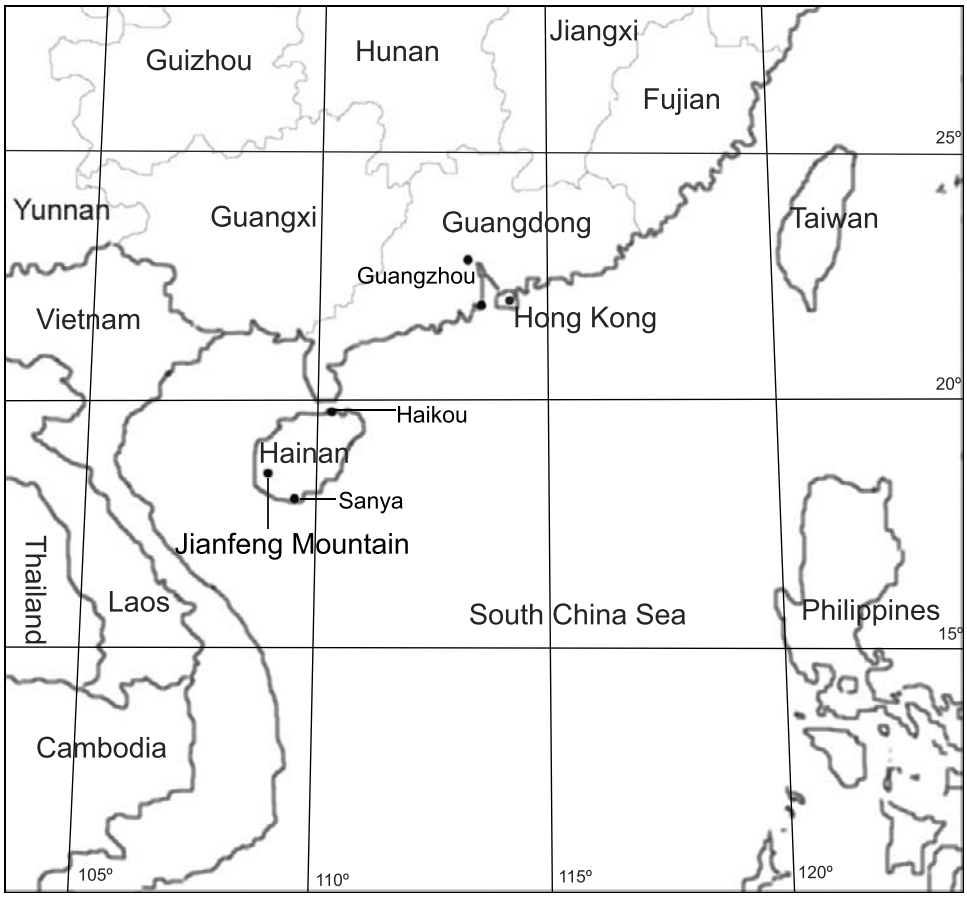

Figure 1. Map showing the sampling site.

presents the analysis of NMHCs data in a tropical forest, a remote site on Hainan Island of south China, with emphasis on the impact due to long-range transport.

2. Experiment

[4] Jianfeng Mountain (18°40′N, 108°49′E) is located on the southwest coast of Hainan Island, at about 120 km from Sanya (with a population of about 482,000), the second largest city of Hainan province, and 320 km from Haikou (with a population of about 830,000), the capital city of Hainan province (Figure 1). The mountain faces the South China Sea in the south and west direction. The sampling site is situated within the Jianfengling National Reserve, which is the second largest tropical rain forest in China with a total area of 475 km^2. The elevation of the sampling site is about 820 m above sea level (ASL). It is surrounded by several hills with heights exceeding 1000 m ASL.

[5] Air samples were collected at the rooftop of a building (field observational station operated by the Chinese Academy of Forest) using prevacuated 2-L stainless steel electropolished canisters provided by University of California, Irvine (UCI). Prior to vacuation, the canisters were cleaned by humidified pure nitrogen gas to inactive the inner surface. A flow controlling device was put on the inlet of each canister to obtain 1-hour integrated air sample. In spring (April and May) and autumn and early winter (1 September $\sim$ 4 December) of 2004, 90 samples and 76 samples were collected, respectively. Most samples were collected at 1200 local time. Additional samples were collected during the intensive study periods (17–24 April, 13–20 May and 3–8 November), in which 5 samples were collected at 0800, 1100, 1400, 1700 and 2000 local time each day. The springtime samples were analyzed by the Research Center for Environmental Changes (RCEC), Academia Sinica, Taiwan, while the other samples were analyzed by UCI.

[6] The RCEC system was derived from the UCI system and they have similar configuration and calibration method. The details of analytical procedures employed in this study can be found in the works by *Blake et al.* [1996, 1997], *Colman et al.* [2001] and *Chang et al.* [2003]. In the RCEC, an automated GC-MS/FID system with two columns (a PLOT and a DB-1) was used to analyze C_2–C_{10} hydrocarbons. The detection limit for C_2–C_{10} hydrocarbons is 15 pptv, and the precision of the measurement is 5% [*Chang et al.*, 2003]. In the UCI, a six-columns multiple GC-MS/FID/ECD system was used to identify and quantify NMHCs and other trace gases. The detection limit for C_2–C_{10} hydrocarbons is 5 pptv. The precision of the measurement varies by compounds and by mixing ratio. For example, it is

1% (or 1.5 pptv) for alkanes and alkyne, and 3% (or 3 pptv) for alkenes [*Colman et al.*, 2001].

3. Result and Discussion

3.1. General Characteristics of NMHCs in Spring and Autumn

[7] The average concentrations of selected C_2-C_7 hydrocarbons for the two seasons are shown in Table 1. The hydrocarbons listed in Table 1 accounted for about 90% of the total mixing ratio of speciated C_2-C_{10} hydrocarbons measured. In this study, only samples collected at 1100–1500 local time were included in the data set for a fair comparison with other studies. Table 1 also shows the OH reaction rate constant [*Atkinson and Arey*, 2003] and lifetime of these hydrocarbons in the atmosphere based on an annual global mean OH concentration of 1.16×10^6 molecules cm^{-3} [*Spivakovsky et al.*, 2000]. Ethane, ethyne and isoprene are the three most abundant hydrocarbons in this site in both seasons. Ethane and ethyne can be from various sources, among which incomplete combustion, such as burnings of fossil fuel, biomass/biofuel including agricultural residues and coal, are the major sources [*Choi et al.*, 2003]. They have relatively long atmospheric lifetimes in the troposphere (Table 1). Thus they can be transported to remote areas far away from the source regions. They are also reported to be the two dominant hydrocarbons in most rural and remote sites [*Saito et al.*, 2000; *Sharma et al.*, 2000; *Wang et al.*, 2003, 2004]. Isoprene is a major biogenic hydrocarbon [*Guenther et al.*, 1995]. Because of the very short lifetime in the atmosphere (Table 1), its major source is local vegetation emission. The dominance of the two long-lived species based on mixing ratios in this remote site, Jianfeng Mountain, indicates that the major sources of NMHCs in this site are from long-range transport of pollutants. The mixing ratios of some hydrocarbons show large variations. This can be attributed to the fact that the sampling site is a remote clean site and there were differences in the accumulation, dilution, and the residence time of hydrocarbons during the long-range transport from the source regions while traveling different pathways.

[8] Compared to the rural sites of Japan, the USA and other rural sites of China in the higher latitudes, most hydrocarbons showed lower concentrations in Jianfeng Mountain except for those measured in autumn at Happo, Japan (Table 1). Happo is a mountainous site in the center of Japan Islands, and is free of local anthropogenic emission [*Sharma et al.*, 2000]. The mixing ratios of most hydrocarbons in Jianfeng Mountain were higher in autumn but lower in spring than those in Happo. This phenomenon illustrates that Jianfeng Mountain was affected by the long-range transport of pollutants from the upwind urban and industrial region of SE China in autumn. Otherwise, the mixing ratios in Happo should be higher since the latitude of Happo is higher than Jianfeng Mountain, and thus the lifetimes of hydrocarbons in Happo should be longer because of the low level of OH radical [*Sharma et al.*, 2000]. Hok Tsui is a relatively clean site in Hong Kong, but it is still affected by short-range transport from the nearby urban area (about 10 km), especially in spring under the prevailing east-northeast flow [*Wang et al.*, 2003]. The concentrations of most hydrocarbons, such as ethane, ethyne, propane and toluene, were several times higher in Hok Tsui than in Jianfeng Mountain in spring (Table 1). Lin'an is a rural site in the Yangtze River Delta region, one of the most industrialized and urbanized region in China [*Guo et al.*, 2004]. Almost all species, such as toluene, ethene and benzene, showed mixing ratios several times higher at the Lin'an site than at Jianfeng Mountain in autumn (Table 1). Hence the low NMHC concentrations in Jianfeng Mountain area, especially when it is not affected by transported air masses, suggest that this site is not significantly impacted by local anthropogenic pollution. Therefore it is an appropriate site for the assessment of the impact of long-range transport of air pollutants from various source regions.

3.2. Local Emission and Diurnal Variation of Isoprene

[9] Local emission from the tropical rain forest is the major source of isoprene. Figure 2 shows the diurnal variations of isoprene in April, May and November. Isoprene showed a strong diurnal cycle in these three months. The diurnal variation of isoprene in November is different from those in April and May. In November, the peak hour occurred at 1100–1200 local time. While in April and May, it occurred at 1400–1500 local time. The diurnal biogenic emission of isoprene is affected mostly by sunlight and temperature [*Kesselmeier and Staudt*, 1999]. Unfortunately, we had not recorded the light intensity and temperature during the sampling periods. So we can only offer an argument for this phenomenon. After sunrise, both radiation intensity and temperature increase, and the biogenic emission of isoprene is activated. It reaches its full strength near 1400 local time in spring. As the reactions of isoprene with OH radical and ozone are temperature-dependent also, and the level of OH and ozone increase with available radiation, the photochemical destruction of isoprene increases with the increase of radiation. The isoprene level is thus reduced and starts to fall. In autumn (October and November) of south China, strong sunlight and photochemical reaction are commonly found in the afternoon [*Wang et al.*, 2001] and isoprene is destructed by photochemical reactions at a faster rate from noon onward. Hence isoprene concentration started to fall at a fast rate after noon.

[10] The average mixing ratios of isoprene at the four rural sites of southeast United States were in the same order as those in Jianfeng Mountain (Table 1), whereas in four rural sites of Canada, the levels of isoprene (0.01–0.20 ppbv in October and November) were much lower than at Jianfeng Mountain [*Bottenheim and Shepherd*, 1995]. At a remote tropical forest site in central Amazonia, levels of isoprene (between 4 and 8 ppbv in March and April) were much higher than at Jianfeng Mountain [*Kesselmeier et al.*, 2000], and at the boundary layer of tropical forests of Surinam in South America, the mean average mixing ratios of isoprene were 2.6 ppbv (in March 1998), which were also much higher than that at Jianfeng Mountain [*Crutzen et al.*, 2000]. In another tropical forest site of southwest China, the levels of isoprene (about 1.5–3.5 ppbv between 1200 and 2000 local time in July) were also higher than that at Jianfeng Mountain [*Baker et al.*, 2005]. There are several factors that affect biogenic isoprene emission, such as plant species and vegetation types, available photosynthetic active radiation (PAR), atmospheric temperature, water stress and phenology [*Kesselmeier and Staudt*, 1999]. Without

Table 1. Average Mixing Ratios (Mean ± S. D.) of Selected Species in Jianfeng Mountain and Comparison With Other Rural Sites[a]

	Jianfengling[b]		Alabama,[c]	Mississipi,[c]	Georgia,[c]	North Carolina,[c]	Chichijima,[d]	Happo[e]		Lin'an[f]		Hok Tsui,[g]		Lifetime,[i]
	Spring	Autumn	Autumn	Autumn	Autumn	Autumn	Winter	Spring	Autumn	Autumn	Spring	Spring	K_{OH}[h]	days
Ethane	0.81 ± 0.34	1.43 ± 0.65	1.56	1.64	1.21	1.26	1.58	1.74	0.95	3.35	3.11	2.37	0.248	40.2
Propane	0.15 ± 0.10	0.46 ± 0.28	1.41	1.36	1.36	1.26	0.54	0.61	0.49	1.59	1.2	0.81	1.09	9.2
Isobutane	0.06 ± 0.13	0.11 ± 0.08	0.26	0.28	0.24	0.24	0.1	0.13	0.11	0.49	0.39	0.22	2.12	4.7
n-butane	0.10 ± 0.19	0.16 ± 0.12	0.55	0.57	0.60	0.71	0.17	0.22	0.19	0.59	0.43	0.33	2.36	4.2
Isopentane	0.21 ± 0.18	0.17 ± 0.12	0.31	0.31	0.54	0.58	0.08	0.11	0.09	0.19	0.33		3.6	3.2
n-pentane	0.15 ± 0.07	0.09 ± 0.06	0.21	0.19	0.35	0.23	0.05	0.08	0.07	0.17	0.13	0.09	3.80	3.0
Ethene	0.33 ± 0.17	0.48 ± 0.38	0.44	0.54	0.53	0.84	0.17	0.21	0.23	3.07	1.61	0.50	8.52	1.2
Propene	0.12 ± 0.04	0.16 ± 0.46	0.22	0.29	0.27	0.23				0.54	0.28	0.06	26.3	0.4
Isoprene	0.77 ± 0.47	0.50 ± 0.33	0.53	0.53	0.35	0.49	0.08						100	0.1
Ethyne	0.34 ± 0.19	1.05 ± 0.67	0.53	0.62	0.58	0.67	0.45	0.7	0.36	2.6	2.39	1.40	0.90[j]	11.1
Benzene	0.15 ± 0.08	0.29 ± 0.17	0.15	0.13	0.16	2.13	0.12			1.33	0.8	0.49	1.22	8.2
Toluene	0.16 ± 0.13	0.22 ± 0.26	0.15	0.13	0.31	0.32	0.78			2.54	1.5	0.54	5.63	1.8

[a]Unit is ppbv.
[b]Spring and autumn: data collected at 1100–1500 local time.
[c]*Hagerman et al.* [1997]. Samples were collected at 1200–1300 local time, 1993. Unit transforms from ppbC.
[d]*Kato et al.* [2001]. Samples were collected at 0400, 0700, 1300 and 1800 local time, 1999.
[e]*Sharma et al.* [2000]. Samples were collected in spring, 1998–1999.
[f]*Guo et al.* [2004]. Samples were collected at noon between October–November 1999 and March–June 2001.
[g]*Wang et al.* [2003]. Samples were collected at 1200–1300 local time, March–April 2001.
[h]*Atkinson and Arey* [2003] (unit: $\times 10^{12}$ cm^3 molecule^{-1} s^{-1} at 298 K).
[i]Based on global annual mean OH = 1.16×10^6 molecules cm^{-3}, *Spivakovsky et al.* [2000].
[j]*Finlayson-Pitts and Pitts* [2000].

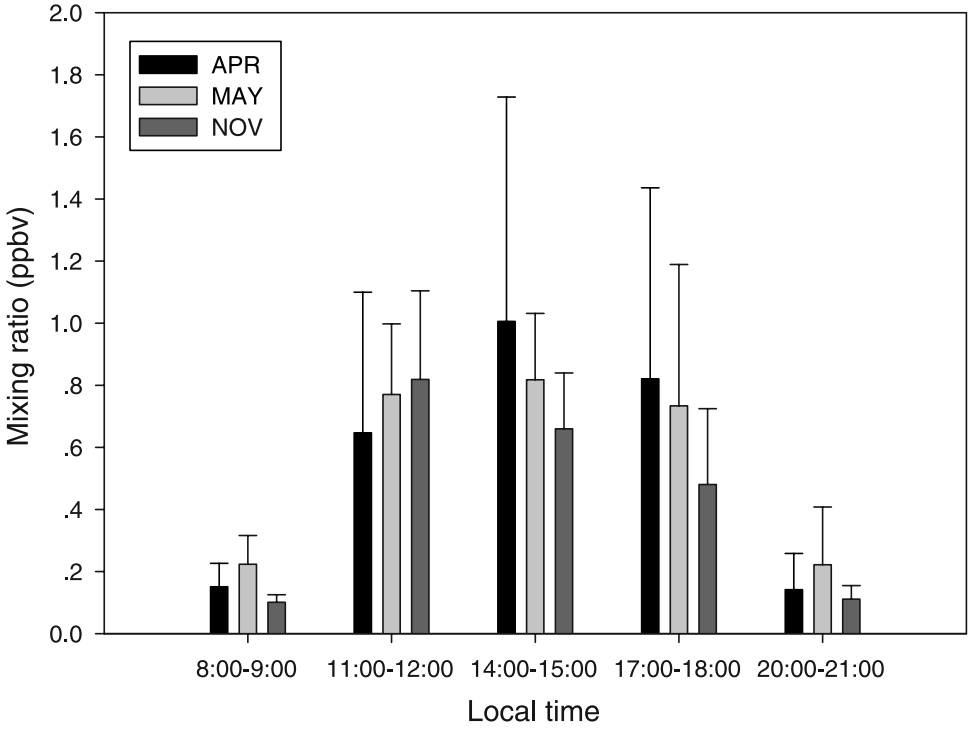

Figure 2. Diurnal variations of isoprene in the three intensive study months.

details information about these parameters, we are not able to tell the causes of the differences in isoprene levels. Also, the levels of isoprene in spring were nearly 60% higher than in autumn at this site, the exact causes of this phenomenon are unclear, and further study is needed to unveil the relevant controlling forces.

[11] Alpha-pinene was also an important biogenic hydrocarbon. However, its mixing ratio measured in this study was very low (with a mean of 0.06 ppbv in spring and 0.03 ppbv in autumn and early winter, respectively) compared to the levels of isoprene. It may be that there is a lack of pinenes-emitter species in this region. Another study on the emission of VOC from tropical forest vegetation of southwest China showed that only a few species emit monoterpene [*Geron et al.*, 2006].

3.3. Characteristics of Long-Range Transport Air Masses

[12] Mixing ratios of ethane, ethyne, and propane observed during PEM-West B (February–March 1994) were on average a factor of 2 larger than those observed during PEM-West A (September–October 1991) [*Talbot et al.*, 1997]. They were attributed to the difference in prevalent winds during the two experimental periods. Air masses from the Asian Continent contained higher mixing ratios of hydrocarbons than those from the Pacific. In addition, it was also affected by the longer lifetimes of NMHCs at the lower latitude (<25°N) than at the higher latitude (>25°N). In this study, most hydrocarbons show higher mixing ratios in autumn than in spring, in particular ethane, ethyne, propane and benzene (Table 1). The differences of NMHC levels between the two seasons were more like the situation at the lower latitude of western Pacific regions observed by *Blake et al.* [1997]. They are associated with the change of wind direction. In autumn, the prevailing winds are northeastern, and the air masses passed over SE China, which is the most industrialized and urbanized region in China. While in spring, the prevailing winds are southwestern, and the air masses passed over SE Asia. This region is less developed than SE China, and active biomass burning are commonly found in spring time because of the slash-and-burn agriculture activities.

[13] Figure 3 compares the average mixing ratio of these anthropogenic hydrocarbons together with their standard deviations in different months. For a fair comparison, only samples collected between 1100 and 1500 local time were shown. Generally, most hydrocarbons had the highest mixing ratios in December, and lowest in May. This trend coincided with another study in a rural site of south China where NMHCs show a maximum in autumn-winter and a minimum in summer [*Wang et al.*, 2005].

[14] Backward air mass trajectory analysis is a useful tool to determine the possible transport pathways of air masses. Using the NOAA HYSPLIT model [*Rolph*, 2003], 5-day backward trajectories of the sampled air masses reaching Jianfeng Mountain were calculated. According to the origin of the transport pathways of the air masses, the trajectories were classified into four major categories (Figure 4).

[15] The first category is the coast of east Asia (CEA). Air masses originated from the boundary layer of mainland China and east Asia, and had passed over the coast of southeast China. They experienced a descending motion during the transport to Jianfeng Mountain. The air masses are affected by the fresh or aged plume from the continental urban/industrial area. Most autumn samples (from 24 September to 4 December) are categorized to this type.

[16] The second category is Southeast Asia (SEA). Air masses originated near the surface of Indian Ocean or South

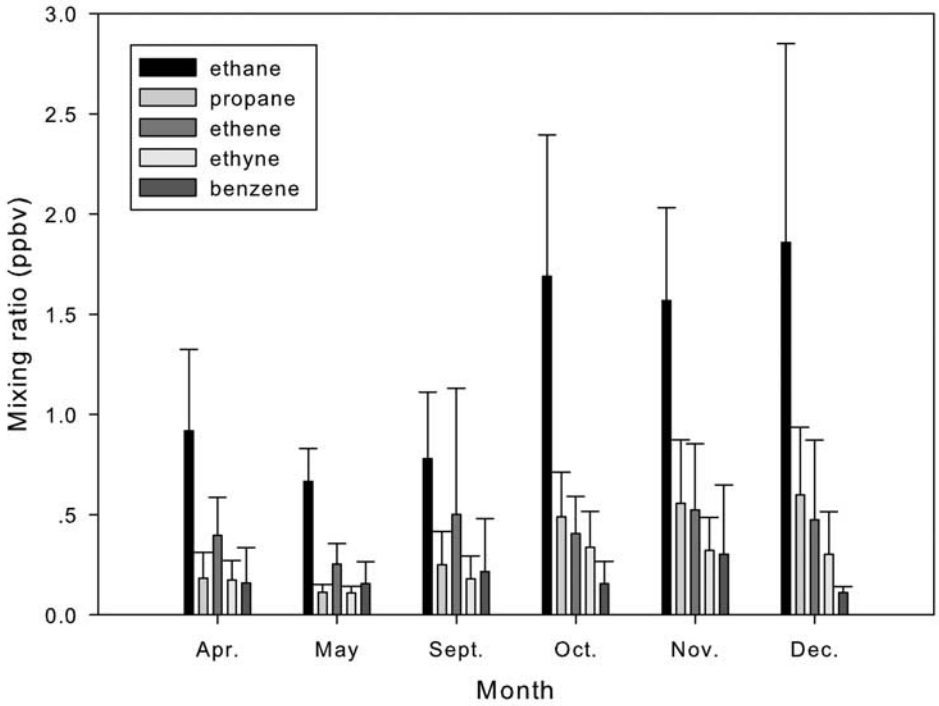

Figure 3. Average mixing ratios together with standard deviation of selected hydrocarbons in different months. Samples were collected at 1100–1500 local time.

China Sea and had passed over the SE Asian continent. They experienced an ascending motion during their transport to Jianfeng Mountain. These air masses are impacted by the emissions from the SE Asian continent. This happened during the periods of 14, 18, and 19 April, 12–14 May and 1–7 September.

[17] The third category is the western Pacific (WP). Air masses originated from the boundary layer of the western Pacific and passed over the tropical and subtropical regions of northwestern Pacific. They experienced a descending motion during their transport to the sampling sites. The samples collected during 15–20 May belong to this type.

[18] The fourth category is the South China Sea (SCS). Air masses originated from the surface of the South China Sea, and had experienced an ascending motion. The samples collected during 16–17 April and 20–24 April are under this category.

[19] In each season, there are several samples with very low mixing ratio of anthropogenic species. Backward trajectory analysis indicates that the air masses in these samples originated from the lower troposphere of the South China Sea and the western Pacific. We classified these samples as spring and autumn background samples respectively.

[20] Table 2 summarizes the average mixing ratios together with standard deviations of selected hydrocarbons in different groups of trajectories in the two seasons. From Table 2, we can see that air masses from CEA in autumn had the highest mixing ratio of most hydrocarbons (such as ethane, ethyne, propane and ethene), compared with those from the other regions. The air masses of CEA group had to pass over large areas of the east Asian coast including highly urbanized and industrialized regions of the Yangtze River Delta, central-eastern China, Taiwan and the Pearl River Delta of SE China. They had picked up industrial/urban pollutants from these regions and hence contained the highest mixing ratios of most long-lived NMHCs. However, because of the long journey, hydrocarbons (for example, propene) with short lifetimes in the atmosphere showed very low mixing ratio in these air masses. Two typical enhancements with obviously higher mixing ratios of ethane, ethene, ethyne and benzene were captured from 18 to 21 October and from 26 to 28 November.

[21] The air masses from SEA in spring are influenced by biomass burning emissions in SE Asia. This is demonstrated by the higher mixing ratios of ethane, ethyne and propane in SEA than in SCS from the ocean. This was also confirmed by the fact that although SEA air masses passed over SE Asia both in spring and autumn, air masses in autumn contained lower mixing ratio of ethane, ethene, propane and ethyne than those in spring because spring is the biomass burning season in SE Asia. The burning activities are believed to emit huge amounts of pollutants including NMHCs, which were transported to downwind regions of the South China Sea and Hainan Island following the prevailing winds. Thus high mixing ratios of NMHCs were observed in the air masses from this region. During 18–20 April, enhanced levels of ethane, propane, ethyne, and ethene were detected even at night. This phenomenon may indicate that the pollutants were elevated on a regional scale.

[22] We also noted that the mixing ratios of many species including propane, isobutene, n-butane, ethane, propene, ethyne and benzene had the lowest mixing ratios in the air mass from WP in spring. This reflects the fact that there are

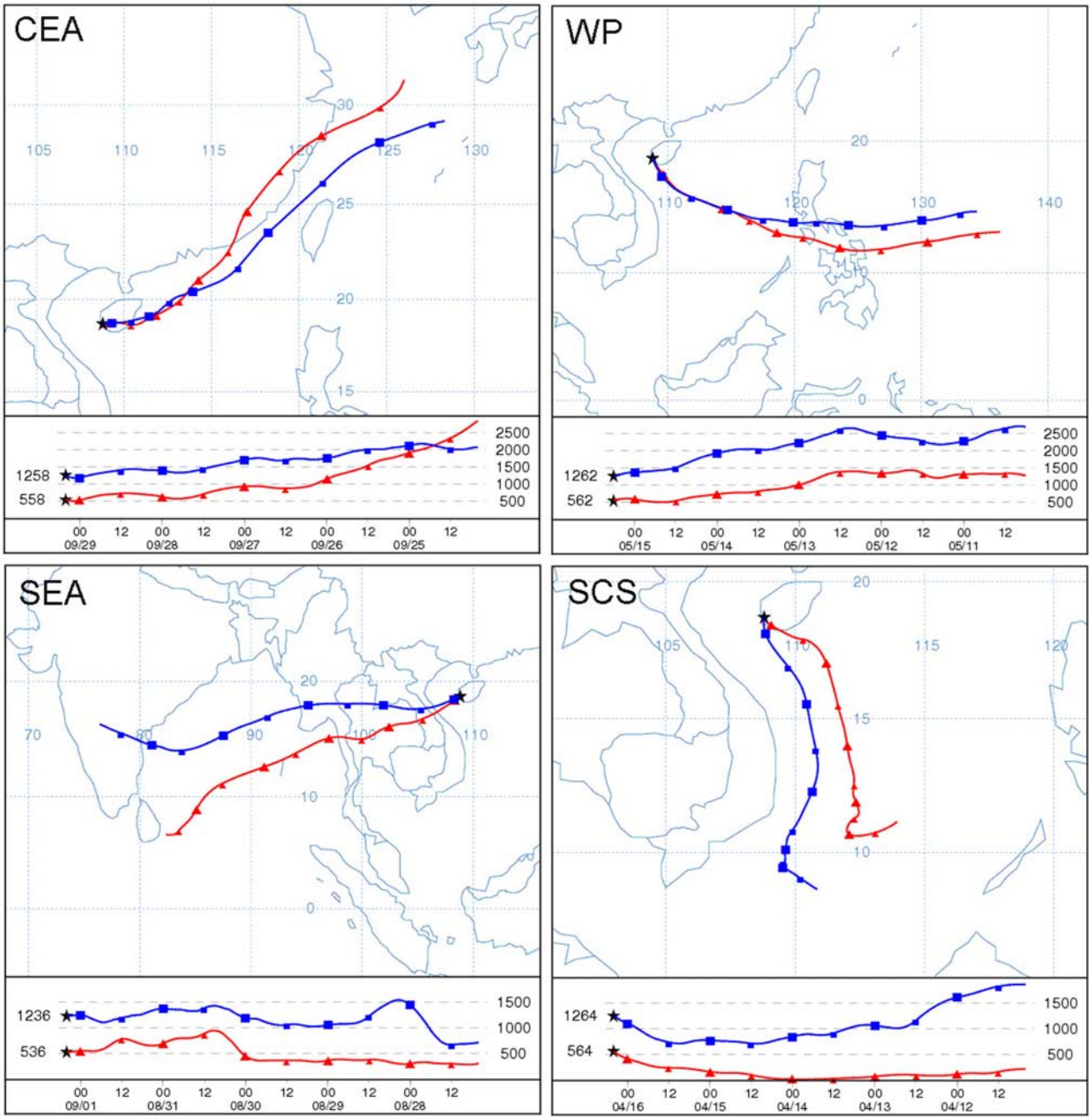

Figure 4. Representative trajectories in different trajectory groups.

no significant man-made sources of air pollutants over the Pacific region.

[23] Table 3 compared the average mixing ratios of selected hydrocarbons during the observed enhanced days to the background samples in the same seasons. Most hydrocarbons showed several times higher mixing ratio in these enhanced days than in the background days. However, the composition of hydrocarbons in these enhancements varied remarkably. This reflects the source characteristics.

[24] Figure 5 shows the backward trajectory of 18 April with the air masses passed through most of SE Asia following the south wind and the fire count map on 16–18 April for the SE Asian region. The fire counts were detected by MODIS (Moderate Resolution Imaging Spectroradiometer) on the NASA satellites and the integrated data are available at the Web site of the University of Maryland (http://maps.geog.umd.edu/products.asp). One fire point in the map represents an active fire in a 1 × 1 km pixel. On these days, the air masses passed through the regions of Vietnam, Cambodia, and Laos and to a lesser extent eastern Thailand, where active biomass burning occurred. Ethane, ethyne, ethene and propane are the dominant hydrocarbons which contributed to 65% of the total NMHCs. n-Butane and propane are the most enhanced hydrocarbons in biomass burning plume compared to the spring background samples. These species are the charac-

Table 2. Average Mixing Ratios Together With Standard Deviations of Selected Species in Different Trajectory Groups[a]

	Spring			Autumn	
	WP (n = 8)[b]	SEA (n = 10)	SCS (n = 13)	CEA (n = 39)	SEA (n = 5)
Ethane	0.59 ± 0.09	1.00 ± 0.36	0.69 ± 0.16	1.63 ± 0.59	0.63 ± 0.18
Propane	0.10 ± 0.03	0.19 ± 0.10	0.12 ± 0.08	0.54 ± 0.27	0.16 ± 0.06
Isobutane	0.03 ± 0.01	0.04 ± 0.02	0.09 ± 0.21	0.13 ± 0.08	0.04 ± 0.03
n-butane	0.05 ± 0.02	0.06 ± 0.03	0.15 ± 0.31	0.19 ± 0.12	0.07 ± 0.03
Isopentane	0.27 ± 0.07	0.16 ± 0.07	0.12 ± 0.05	0.18 ± 0.11	0.18 ± 0.18
n-pentane	0.17 ± 0.05	0.14 ± 0.05	0.11 ± 0.02	0.10 ± 0.06	0.05 ± 0.03
Ethene	0.26 ± 0.11	0.33 ± 0.16	0.37 ± 0.22	0.48 ± 0.28	0.26 ± 0.11
Propene	0.10 ± 0.02	0.10 ± 0.03	0.14 ± 0.05	0.08 ± 0.05	0.18 ± 0.10
Isoprene	0.81 ± 0.17	0.54 ± 0.40	0.99 ± 0.59	0.51 ± 0.34	0.36 ± 0.24
Ethyne	0.21 ± 0.07	0.41 ± 0.21	0.30 ± 0.09	1.23 ± 0.64	0.31 ± 0.09
Benzene	0.10 ± 0.02	0.18 ± 0.09	0.12 ± 0.03	0.33 ± 0.16	0.12 ± 0.04
Toluene	0.13 ± 0.02	0.13 ± 0.04	0.16 ± 0.20	0.23 ± 0.26	0.22 ± 0.10
Sum[c]	3.29 ± 0.42	3.57 ± 0.74	3.93 ± 1.06	6.18 ± 2.45	5.03 ± 3.95

[a]Unit is ppbv. Data for the samples collected from 1100 to 1500 local time.
[b]Numbers of samples.
[c]Sum is the total mixing ratio of all hydrocarbons measured and quantified.

teristic hydrocarbons in the biomass burning plume [*Woo et al.*, 2003].

[25] Figure 6 shows the backward trajectory on 19 October with the air masses trespassing the east and SE China following the ENE to NE wind and the fire count map during 16–18 October. The air masses passed through the boundary layer of SE China. In this period, the burning of crop residues after harvest is one of the most important NMHC sources in rural China [*Streets et al.*, 2003b]. High mixing ratios of ethane (2.57 ± 0.33 ppbv) and ethyne (2.25 ± 0.44 ppbv) were found on these days. High ethane is associated with biomass/biofuel burning, but the high ethyne concentration is influenced by additional contribution from vehicular exhaust, as ethyne is a major component of vehicular exhaust. Although ethene is a major pollutant both in the biomass burning and vehicular emission, its concentration is lower compared to that of ethane and ethyne. This is due to the long journey from the source region to the sampling site compared to the short lifetime of ethene in the atmosphere. The lifetime of toluene is as short as ethene in the atmosphere, the average mixing ratio of toluene (0.20 ± 0.13 ppbv) is found to be nearly three times higher than that of the April enhancement (0.07 ± 0.02 ppbv) which is mainly due to biomass burning emission transport. It demonstrates the contribution of anthropogenic emission of toluene in SE China.

[26] In the November enhancement, the highest mixing ratio of propane (1.08 ± 0.07 ppbv) and ethene (1.06 ± 0.44 ppbv) was detected. Figure 7 shows the backward trajectory on 26 November with the air masses trespassed the east and south China coast following the NE wind. The fire count map during 24–26 November is also shown. This is the typical air mass pathway during the November enhancement. In these days, air masses passed through the

Table 3. Comparison of the Average Mixing Ratios of Selected Species in Enhanced Days With the Background Average Mixing Ratios[a]

	Spring Background	18–19 Apr	Autumn Background	18–21 Oct	26–28 Nov
Ethane	0.45 ± 0.02	1.33 ± 0.13	1.00 ± 0.10	2.57 ± 0.33	2.44 ± 0.14
Propane	0.05 ± 0.02	0.28 ± 0.05	0.25 ± 0.01	0.74 ± 0.08	1.08 ± 0.07
Isobutane	0.01 ± 0.01	0.06 ± 0.04	0.04 ± 0.01	0.17 ± 0.04	0.28 ± 0.03
n-butane	0.02 ± 0.01	0.15 ± 0.20	0.06 ± 0.02	0.24 ± 0.03	0.43 ± 0.04
Isopentane	0.25 ± 0.05	0.14 ± 0.09	0.05 ± 0.02	0.19 ± 0.06	0.26 ± 0.13
n-pentane	0.16 ± 0.04	0.13 ± 0.05	0.03 ± 0.01	0.12 ± 0.03	0.19 ± 0.04
Ethene	0.15 ± 0.01	0.47 ± 0.19	0.23 ± 0.01	0.61 ± 0.19	1.06 ± 0.44
Propene	0.09 ± 0.02	0.13 ± 0.04	0.03 ± 0.00	0.11 ± 0.04	0.07 ± 0.05
Isoprene	0.08 ± 0.08	0.20 ± 0.15	0.09 ± 0.02	0.79 ± 0.34	0.22 ± 0.17
Ethyne	0.06 ± 0.02	0.64 ± 0.12	0.49 ± 0.06	2.25 ± 0.44	2.19 ± 0.39
Benzene	0.06 ± 0.01	0.25 ± 0.03	0.16 ± 0.03	0.56 ± 0.09	0.60 ± 0.15
Toluene	0.08 ± 0.02	0.12 ± 0.04	0.05 ± 0.03	0.20 ± 0.13	0.61 ± 0.51
Sum[b]	1.67 ± 0.13	4.34 ± 0.57	2.61 ± 0.05	9.18 ± 1.39	10.58 ± 2.46
C_2H_6/C_3H_8	11.3 ± 5.7	4.9 ± 0.9	4.1 ± 0.6	3.4 ± 0.3	2.2 ± 0.1
C_2H_6/C_2H_2	8.7 ± 3.3	2.1 ± 0.4	2.1 ± 0.1	1.2 ± 0.1	1.1 ± 0.2
C_3H_8/C_6H_6	0.7 ± 0.2	1.1 ± 0.2	1.6 ± 0.2	1.3 ± 0.1	1.8 ± 0.3

[a]Unit is ppbv for hydrocarbons and volume/volume for hydrocarbon ratios.
[b]Sum is the total mixing ratio of all hydrocarbons measured and quantified.

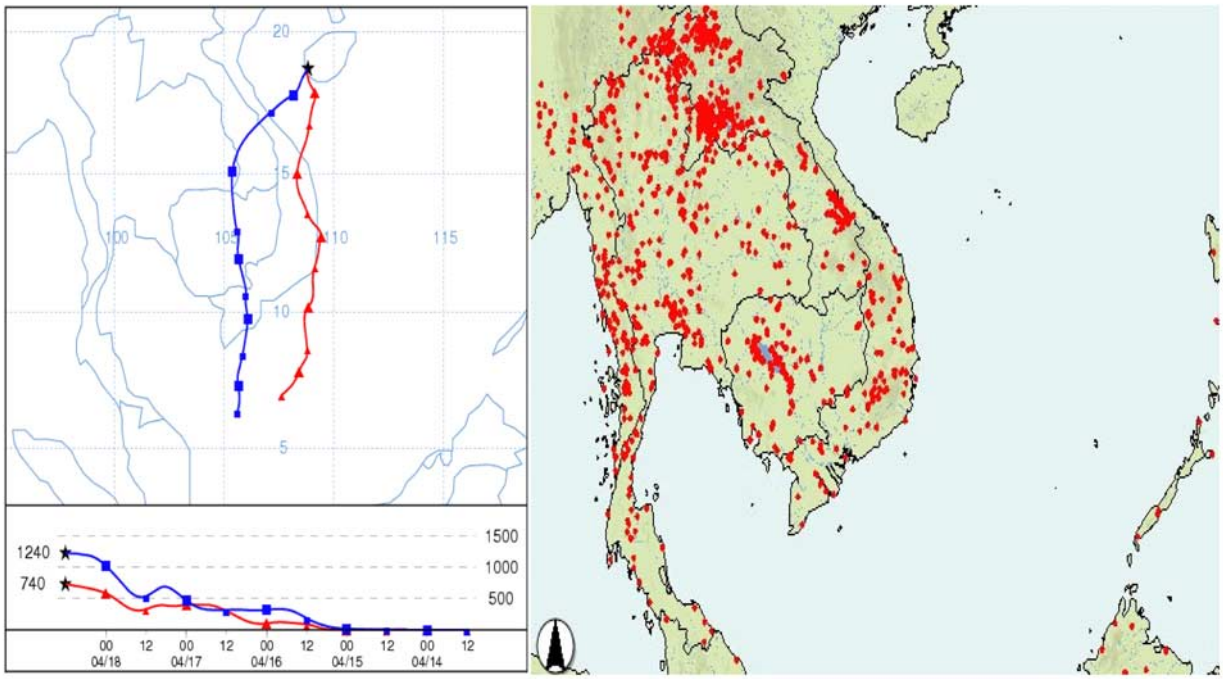

Figure 5. Trajectory on 18 April and fire count map on 16–18 April 2004.

boundary layer of the coast of eastern China, and the Pearl River Delta (PRD), which are major industrial source regions. The higher level of ethene (1.06 ± 0.44 ppbv) in the November enhancement compared to that in October enhancement (0.61 ± 0.19 ppbv) indicates the contribution of urban vehicular emission from PRD urban cities. Because of the short lifetime of ethene, such high mixing ratios typically cannot survive long-range transport from a remote source region. So they are likely originated from local or regional sources. However, mixing ratios of even shorter-

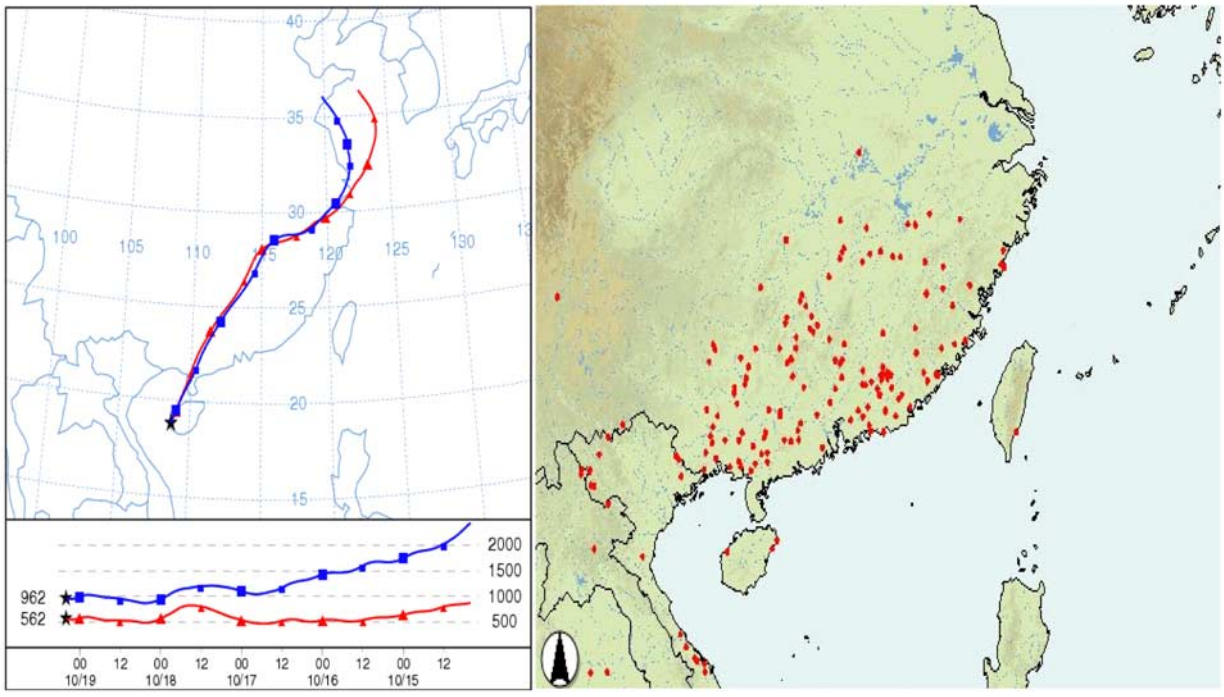

Figure 6. Trajectory on 19 October and fire count map on 16–18 October.

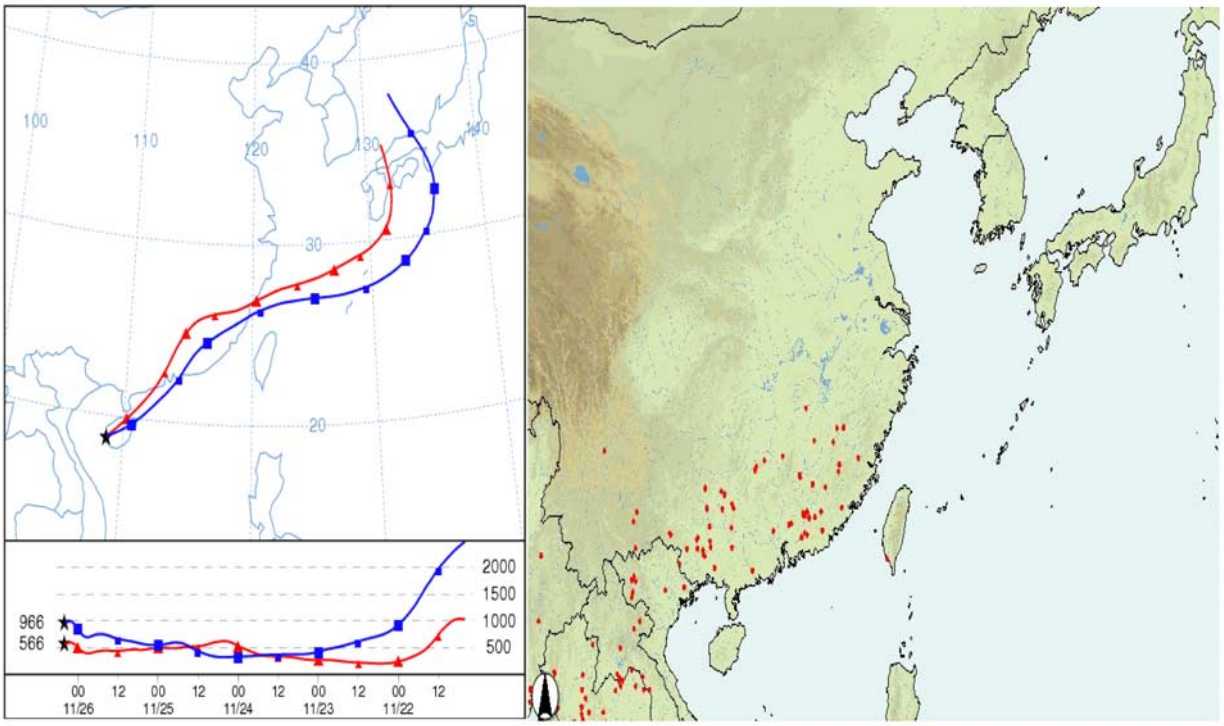

Figure 7. Trajectory on 26 November and fire count map on 24–26 November.

lived propene, which is coemitted with ethene from vehicle exhausts, were low (0.07 ppbv) on the days that ethene was high. This indicates that regional rather than local or remote emissions dominated ethene levels at the sampling site during this period.

3.4. Characteristic Ratios of Long-Range Transport Air Masses

[27] In this section, we further examine source signature ratios, which are presented in Table 3. Both ethane and propane are mostly emitted from anthropogenic sources. Fossil fuel combustion, biomass burning, nature gas and liquefied petroleum gas (LPG) are the major sources of ethane, while nature gas, LPG and biomass burning are the major sources of propane [*Choi et al.*, 2003]. The concentration ratio of ethane to propane is widely used to investigate the emission characteristics of various source regions and the relative age of the air mass [*Talbot et al.*, 1997; *Carmichael et al.*, 2003; *Russo et al.*, 2003; *Wang et al.*, 2003, 2005]. The ratio of ethane/propane (C_2H_6/C_3H_8) was estimated to be 2.1 in China and 3.8 in SE Asia on the basis of the anthropogenic emission inventory [*Russo et al.*, 2003]. *Carmichael et al.* [2003] reported the C_2H_6/C_3H_8 ratio of 8 in the SE Asian biomass burning plumes, 2.3 in biofuel combustion exhaust and 0.5 in traffic affected air. They also reported a ratio of 1 to 6 during the TRACE-P campaign. *Wang et al.* [2003, 2005] found a C_2H_6/C_3H_8 ratio of 2.6–2.7 in the air mass from local urban region and Mainland China, 3.1 from the coast of Mainland China at Hok Tsui, 2.7 at Lin'an (a rural site in eastern China) and 1.6 at Tai O (a rural site of Hong Kong). In this study, the C_2H_6/C_3H_8 ratio was 4.6 ± 0.8 in the April enhancement (17–18 April), 3.4 ± 0.3 in the October enhancement and 2.2 ± 0.1 in the November enhancement. The highest ratio of C_2H_6/C_3H_8 (4.6) in air masses from SE Asia is associated with biomass burning emission. In addition, the increasing use of LPG in vehicles and domestic use in the more developed regions (e.g., PRD) results in the lowering of the C_2H_6/C_3H_8 ratio. A low ratio (1.6) was observed in Tai O as its air is more impacted by the fresh plume from the Hong Kong urban region. We also observed lower ratios in the air masses during the October enhancement and November enhancement periods when air masses passed through east coastal China, especially through the PRD region.

[28] *Carmichael et al.* [2003] found that the observed propane/benzene ratios during the TRACE-P period matched well with the calculated ratios based on the emission inventory in China. Propane and benzene have close atmospheric lifetime against OH (9.2 and 8.2 days, respectively, Table 1). In the absence of mixing with other air masses from different sources, the ratio of benzene to propane remains unchanged after emission. Thus the ratio may reflect the source signatures. The April and October propane/benzene ratios (Table 3) fall within the observed ratios (<1.6) for SE Asia reported by *Carmichael et al.* [2003]. It is also close to the ratios found in the other two rural sites of China: Linan (1.4) and Tai O (1.4) [*Wang et al.*, 2005]. In the November enhancement, the C_3H_8/C_6H_6 ratio lies within the observation in southeast China (1.6–2.0) during the TRACE-P campaign [*Carmichael et al.*, 2003].

[29] One major source of ethyne is incomplete fossil fuel combustion, such as vehicle exhaust. It is the dominant

species in roadside samples in PRD region [*Chan et al.*, 2006]. The ethane/ethyne ratio thus reflects the degree of urban vehicular contribution to the air masses. In the October and November enhancements, the ratios were 1.2 ± 0.1 and 1.1 ± 0.2, respectively, compared to 2.0 ± 0.4 in the April enhancement. In the outflow from south China, which passed through the Hong Kong urban region, the value was 0.8 at Tai O, Hong Kong [*Wang et al.*, 2005]. The low value of this ratio indicates the contribution of ethyne from urban vehicular emission.

4. Conclusion

[30] This study investigated the impacts of air masses transported from long range/region (e.g., coastal China emission) on the NMHC profile at a remote tropical forest site in Hainan Island, south China, and they were compared with the impact of local emissions. Jianfeng Mountain is a good site for assessing the impacts of long-range transport of industrial/urban air pollutants in south China as well as biomass burning pollutants in SE Asia, as there are very limited local anthropogenic sources of hydrocarbons. In the two seasons, NMHCs show different patterns. In spring, biomass burning emission in SE Asia contributed significantly to the NMHC mixing ratio under the prevailing southwest wind. In the biomass burning plumes, high mixing ratios of ethane, ethyne, propane and ethene were observed and compared to the ratios from background air masses. In autumn, the long-range transport of anthropogenic pollutants from SE China was the major source. Pollutant sources are fossil fuel combustion, LPG leakage, industrial solvent evaporation and vehicular emission. The high level of toluene in October and November enhancements reflect the contribution from industrial solvent use. The high levels of ethane and ethyne in the October enhancement are attributed to autumn harvesting biomass burning in addition to industrial and urban source emission, while the high levels of ethene in November enhancement is attributed to picking up of vehicular emission when traveling through the PRD urban region. Apart from long-range pollutants transported to this site, the sampling location was relatively free of short-range/local anthropogenic emissions. Isoprene is the most abundant hydrocarbon emitted from local biogenic sources which showed strong diurnal variations in spring and autumn. However, the levels of isoprene in this site are lower than other tropical forest sites, and the exact reasons need to be further explored.

[31] The high C_2H_6/C_3H_8 ratios observed for SE Asia air masses was indicative of a large contribution from biomass burning emissions. A C_3H_8/C_6H_6 ratio of around 1.8 in the November air masses from coast of east Asia reflects the impact of fuel combustion in the south China region, while the low C_2H_6/C_2H_2 ratio reflects the contribution from the urban vehicle exhaust. These ratios are good indicators of source region characteristics.

[32] **Acknowledgments.** This project is funded by the Research Grants Council of Hong Kong (PolyU 5048/02E and PolyU 5131/04E) and a research grant of the Hong Kong Polytechnic University (A504). We would like to acknowledge the contribution of the Administration of Jianfengling Nature Reserve and all the staff who participated in the field sampling. We thank Wang Xinming of the State Key Laboratory of Organic Geochemistry of Chinese Academy of Sciences for his helpful comments. Thanks also go to D. R. Blake and his research group members for chemical analysis. The suggestions of anonymous reviewers have greatly improved the quality of this manuscript and are sincerely appreciated.

References

Atkinson, R., and J. Arey (2003), Atmospheric degradation of volatile organic compounds, *Chem. Rev.*, *103*, 4605–4638.

Baker, B., et al. (2005), Wet and dry season ecosystem level fluxes of isoprene and monoterpenes from a southeast Asian secondary forest and rubber tree plantation, *Atmos. Environ.*, *39*, 381–390.

Blake, D. R., T. Chen, T. W. Smith, C. J. L. Wang, O. W. Wingenter, N. J. Blake, and F. S. Rowland (1996), Three-dimensional distribution of nonmethane hydrocarbons and halocarbons over the northwestern Pacific during the 1991 Pacific Exploratory Mission (PEM-West A), *J. Geophys. Res.*, *101*, 1763–1778.

Blake, N. J., D. R. Blake, T. Chen, J. E. Collins, G. W. Sachse, B. E. Anderson, and F. S. Rowland (1997), Distribution and seasonality of selected hydrocarbons and halocarbons over the western Pacific basin during PEM-West A and PEM-West B, *J. Geophys. Res.*, *102*, 28,315–28,331.

Blake, N. J., et al. (2003), NMHCs and halocarbons in Asian continental outflow during the Transport and Chemical Evolution over the Pacific (TRACE-P) field campaign: Comparison with PEM-West B, *J. Geophys. Res.*, *108*(D20), 8806, doi:10.1029/2002JD003367.

Bottenheim, J. W., and M. F. Shepherd (1995), C_2–C_6 hydrocarbon measurements at four rural locations across Canada, *Atmos. Environ.*, *29*, 647–664.

Carmichael, G. R., et al. (2003), Evaluating regional emission estimates using the TRACE-P observations, *J. Geophys. Res.*, *108*(D21), 8810, doi:10.1029/2002JD003116.

Chan, C. Y., L. Y. Chan, J. M. Harris, S. J. Oltmans, D. R. Blake, Y. Qin, Y. G. Zheng, and X. D. Zheng (2003), Characteristics of biomass burning emission sources, transport, and chemical speciation in enhanced springtime tropospheric ozone profile over Hong Kong, *J. Geophys. Res.*, *108*(D1), 4015, doi:10.1029/2001JD001555.

Chan, L. Y., C. Y. Chan, H. Y. Liu, S. Christopher, S. Oltmans, and J. M. Harris (2000), A case study on the biomass burning in Southeast Asia and enhancement of tropospheric ozone over Hong Kong, *Geophys. Res. Lett.*, *27*(10), 1479–1482.

Chan, L.-Y., K.-W. Chu, S.-C. Zou, C.-Y. Chan, X.-M. Wang, B. Barletta, D. R. Blake, H. Guo, and W.-Y. Tsai (2006), Characteristics of nonmethane hydrocarbons (NMHCs) in industrial, industrial-urban, and industrial-suburban atmospheres of the Pearl River Delta (PRD) region of south China, *J. Geophys. Res.*, *111*, D11304, doi:10.1029/2005JD006481.

Chang, C. C., S. J. Lo, J. G. Lo, and J. L. Wang (2003), Analysis of methyl tert-butyl ether in the atmosphere and implications as an exclusive indicator of automobile exhaust, *Atmos. Environ.*, *37*, 4747–4755.

Choi, Y., S. Elliott, I. J. Simpson, D. R. Blake, J. J. Colman, M. K. Dubey, S. Meinardi, F. S. Rowland, T. Shirai, and F. A. Smith (2003), Survey of whole air data from the second airborne Biomass Burning and Lightning Experiment using principal component analysis, *J. Geophys. Res.*, *108*(D5), 4163, doi:10.1029/2002JD002841.

Colman, J. J., A. Swanson, S. Meinardi, B. C. Sive, D. R. Blake, and F. S. Rowland (2001), Description of the analysis of a wide range of volatile organic compounds in whole air samples collected during PEM-Tropics A and B, *Anal. Chem.*, *73*, 3723–3731.

Crutzen, P. J., et al. (2000), High spatial and temporal resolution measurements of primary organics and their oxidation products over the tropical forests of Surinam, *Atmos. Environ.*, *34*, 1161–1165.

de Gouw, J. A., et al. (2004), Chemical composition of air masses transported from Asia to the U.S. West Coast during ITCT 2K2: Fossil fuel combustion versus biomass-burning signatures, *J. Geophys. Res.*, *109*, D23S20, doi:10.1029/2003JD004202.

Duncan, B. N., R. V. Martin, A. C. Staudt, R. Yevich, and J. A. Logan (2003), Interannual and seasonal variability of biomass burning emissions constrained by satellite observations, *J. Geophys. Res.*, *108*(D2), 4100, doi:10.1029/2002JD002378.

Finlayson-Pitts, B. J., and J. N. Pitts Jr. (Eds.) (2000), *Chemistry of the Upper and Lower Atmosphere: Theory, Experiments, and Applications*, 206 pp., Academic, San Diego, Calif.

Geron, C., S. Owen, A. Guenther, J. Greenberg, R. Rasmussen, J. H. Bai, Q. J. Li, and B. Baker (2006), Volatile organic compounds from vegetation in southern Yunan province, China: Emission rates and some potential regional implications, *Atmos. Environ.*, *40*, 1759–1773.

Guenther, A., et al. (1995), A global model of natural volatile organic compound emissions, *J Geophys. Res.*, *100*, 8873–8892.

Guo, H., et al. (2004), Source contributions to ambient VOCs and CO at a rural site in eastern China, *Atmos. Environ.*, *38*, 4551–4560.

Hagerman, L. M., V. P. Aneja, and W. A. Lonneman (1997), Characterization of non-methane hydrocarbons in the rural southeast United States, *Atmos. Envion.*, *31*, 4017–4038.

Heald, C. L., D. J. Jacob, P. I. Palmer, M. J. Evans, G. W. Sachse, H. B. Singh, and D. R. Blake (2003), Biomass burning emission inventory with daily resolution: Application to aircraft observations of Asian outflow, *J. Geophys. Res.*, *108*(D21), 8811, doi:10.1029/2002JD003082.

Houweling, S., F. Dentener, and J. Lelieveld (1998), The impact of nonmethane hydrocarbon compounds on tropospheric photochemistry, *J. Geophys. Res.*, *103*, 10,673–10,696.

Ito, A., and J. E. Penner (2004), Global estimates of biomass burning emissions based on satellite imagery for the year 2000, *J. Geophys. Res.*, *109*, D14S05, doi:10.1029/2003JD004423.

Jacob, D. J., J. H. Crawford, M. M. Kleb, V. S. Connors, R. J. Bendura, J. L. Raper, G. W. Sachse, J. C. Gille, L. Emmons, and C. L. Heald (2003), Transport and chemical evolution over the Pacific (TRACE-P) aircraft mission: Design, execution, and first results, *J. Geophys. Res.*, *108*(D20), 9000, doi:10.1029/2002JD003276.

Kato, S., P. Pochanart, and Y. Kajii (2001), Measurements of ozone and nonmethane hydrocarbons at Chichi-jima island, a remote island in the western Pacific: Long-range transport of polluted air from the Pacific rim region, *Atmos. Environ.*, *35*, 6021–6029.

Kesselmeier, J., and M. Staudt (1999), Biogenic volatile organic compounds (VOC): An overview of emission, physiology and ecology, *J. Atmos. Chem.*, *33*, 23–88.

Kesselmeier, J., et al. (2000), Atmospheric volatile organic compounds (VOC) at a remote tropical forest site in central Amazonia, *Atmos. Environ.*, *34*, 4063–4072.

Poisson, N., M. Kanakidou, and P. J. Crutzen (2000), Impact of nonmethane hydrocarbons on tropospheric chemistry and the oxidizing power of the global troposphere: 3-dimensional modelling results, *J. Atmos. Chem.*, *36*, 157–230.

Rolph, G. D., (2003), HYSPLIT model, NOAA Air Resour. Lab., Silver Spring, Md. (Available at http://www.arl.noaa.gov/ready/hysplit4.html)

Russo, R., et al. (2003), Chemical composition of Asian continental outflow over the western Pacific: Results from Transport and Chemical Evolution over the Pacific (TRACE-P), *J. Geophys. Res.*, *108*(D20), 8804, doi:10.1029/2002JD003184.

Saito, T., Y. Yokouchi, and K. Kawamura (2000), Distributions of C_2–C_6 hydrocarbons over the western North Pacific and eastern Indian Ocean, *Atmos. Environ.*, *34*, 4373–4381.

Sharma, U. K., Y. Kaji, and H. Akimoto (2000), Seasonal variation of C_2–C_6 NMHCs at Happo, a remote site in Japan, *Atmos. Environ.*, *34*, 4447–4458.

Spivakovsky, C. M., et al. (2000), Three-dimensional climatological distribution of tropospheric OH: update and evaluation, *J. Geophy. Res.*, *105*(D7), 8931–8980.

Streets, D. G., et al. (2003a), An inventory of gaseous and primary aerosol emissions in Asia in the year 2000, *J. Geophys. Res.*, *108*(D21), 8809, doi:10.1029/2002JD003093.

Streets, D. G., K. F. Yarber, J. H. Woo, and G. R. Carmichael (2003b), Biomass burning in Asia: Annual and seasonal estimates and atmospheric emissions, *Global Biogeochem. Cycles*, *17*(4), 1099, doi:10.1029/2003GB002040.

Talbot, R. W., et al. (1997), Chemical characteristics of continental outflow from Asia to the troposphere over the western Pacific Ocean during February–March 1994: Results from PEM-West B, *J. Geophys. Res.*, *102*(D23), 28,255–28,274.

Wang, T., T. F. Cheung, K. S. Lam, G. L. Kok, and J. M. Harris (2001), The characteristics of ozone and related compounds in the boundary layer of the south China coast: Temporal and vertical variations during autumn season, *Atmos. Environ.*, *35*, 2735–2746.

Wang, T., A. J. Ding, D. R. Blake, W. Zahorowski, C. N. Poon, and Y. S. Li (2003), Chemical characterization of the boundary layer outflow of air pollution to Hong Kong during February–April 2001, *J. Geophys. Res.*, *108*(D20), 8787, doi:10.1029/2002JD003272.

Wang, T., et al. (2004), Relationships of trace gases and aerosols and the emission characteristics at Lin'an, a rural site in eastern China, during spring 2001, *J. Geophys. Res.*, *109*, D19S05, doi:10.1029/2003JD004119.

Wang, T., et al. (2005), Measurements of trace gases in the inflow of South China Sea background air and outflow of regional pollution at Tai O, southern China, *J. Atmos. Chem.*, *52*, 295–317.

Woo, J. H., et al. (2003), Contribution of biomass and biofuel emissions to trace gas distributions in Asia during the TRACE-P experiment, *J. Geophys. Res.*, *108*(D21), 8812, doi:10.1029/2002JD003200.

C.-Y. Chan, L.-Y. Chan, Y.-S. Li, and J.-H. Tang, Department of Civil and Structural Engineering, Hong Kong Polytechnic University, Hung Hom, Kowloon, Hong Kong. (celychan@polyu.edu.hk)

C.-C. Chang and S.-C. Liu, Research Center for Environmental Changes, Academia Sinica, Taipei 115, Taiwan.

Y.-D. Li, Research Institute of Tropical Forestry, Chinese Academy of Forestry, Guangzhou 510520, China.